



Generalised acoustic impedance for viscous fluids

Gwénaél Gabard

► To cite this version:

Gwénaél Gabard. Generalised acoustic impedance for viscous fluids. Journal of Sound and Vibration, 2020, 484, pp.115525 -. 10.1016/j.jsv.2020.115525 . hal-03490878

HAL Id: hal-03490878

<https://hal.science/hal-03490878>

Submitted on 28 Jun 2022

HAL is a multi-disciplinary open access archive for the deposit and dissemination of scientific research documents, whether they are published or not. The documents may come from teaching and research institutions in France or abroad, or from public or private research centers.

L'archive ouverte pluridisciplinaire **HAL**, est destinée au dépôt et à la diffusion de documents scientifiques de niveau recherche, publiés ou non, émanant des établissements d'enseignement et de recherche français ou étrangers, des laboratoires publics ou privés.



Distributed under a Creative Commons Attribution - NonCommercial 4.0 International License

Generalised Acoustic Impedance for Viscous Fluids

Gwénaél Gabard^{a,*}

^aLAUM (UMR CNRS 6613), Le Mans Université, France

Abstract

A general class of acoustic impedance conditions is considered where a linear dependence is assumed between the fluid velocity and the surface traction. In addition to the classical impedance relating pressure and normal velocity, this generalised definition of the impedance includes effects such as the friction along the surface as well as coupling between the normal velocity and the tangential force on the fluid. After providing a generalised definition based on impedance and admittance matrices, various fundamental principles are considered to ensure the impedance is physically admissible. These principles include the reality, causality, stability and passivity of the surface. To illustrate the influence of the additional parameters introduced by the generalised impedance, a number of results are presented for the reflection of a plane wave on a lined surface, with or without a mean flow.

Keywords: acoustic impedance, surface traction, causality, passivity

1. Introduction

In classical acoustics, i.e. for an inviscid fluid, the surface impedance defines a linear relation between the normal fluid velocity and pressure. In the frequency domain, this boundary condition is sufficient to obtain a well-posed problem. In the time domain, the impedance function $Z(\omega)$ should satisfy a number of admissibility constraints, see [1] and [2]. When considering a viscous fluid, more boundary conditions are needed. In addition to the condition on the normal velocity, a no-slip condition is generally applied, stating that the tangential velocity vanishes on the surface. An alternative is to have a zero shear stress along the surface.

Standard impedance models, such as those from Rienstra [1] or Tam & Auriault [3], do not provide any information on the behaviour of the tangential component of velocity at the surface. When applied to viscous flows, and in the absence of more information, these impedance models are generally complemented with the no-slip condition [4, 5, 6]. Prompted by inconsistencies observed in the impedance deduced from measurements with flow [7], it has been recently suggested that additional parameters should be introduced to fully characterize an acoustic treatment under a grazing flow. One such parameter is the momentum transfer impedance relating the tangential force on the surface and the normal velocity [8]. Another option is the introduction of a friction coefficient [9]. Another mechanism under consideration is the coupling with the hydrodynamic field [10].

In this paper we consider a general class of impedance boundary conditions where a linear dependence is posited between the surface traction and the fluid velocity. In Section 2, these boundary conditions are formulated both in the time domain and the frequency domain. They provide a unified framework to describe a large group of boundary conditions, including the momentum transfer impedance. In Section 3, a number of conditions on the generalised impedance are derived in order to obtain an admissible physical model, namely the reality, causality, stability and passivity of the impedance. The two-dimensional case is considered in more details and results for the reflection of a plane wave are presented.

*Correspondence to: Gwénaél Gabard, LAUM, Le Mans Université, Avenue Olivier Messiaen, 72085 Le Mans, France. gwenael.gabard@univ-lemans.fr

2. Generalised Acoustic Impedance

We consider a compressible, viscous fluid in contact with a surface Γ . The surface traction (i.e. the surface force) induced on the surface by the fluid is given by $\mathbf{t} = -\boldsymbol{\sigma} \cdot \mathbf{n}$, where $\boldsymbol{\sigma}$ is the Cauchy stress tensor and \mathbf{n} is the unit normal vector pointing into the surface. For a Newtonian fluid, we will use the constitutive relation $\boldsymbol{\sigma} = -p\mathbf{I} + \boldsymbol{\tau}$, where p is the pressure, \mathbf{I} is the identity tensor and $\boldsymbol{\tau}$ is the tensor of viscous stresses. It follows that $\mathbf{t} = p\mathbf{n} - \boldsymbol{\tau} \cdot \mathbf{n}$.

2.1. Time domain

To generalise the concept of acoustic impedance, we assume a linear dependence between the surface traction \mathbf{t} and the fluid velocity \mathbf{u} on the surface:

$$\mathcal{P}[\mathbf{u}, \mathbf{x}, \mathbf{n}](t) = \mathcal{Q}[\mathbf{t}, \mathbf{x}, \mathbf{n}](t), \quad (1)$$

where \mathcal{P} and \mathcal{Q} are two linear differential operators. \mathbf{x} is the position along the surface Γ . We will assume that the operators \mathcal{P} and \mathcal{Q} only involves \mathbf{u} and \mathbf{t} as well as their time derivatives but do not involve their spatial derivatives. In addition, if the surface is uniform, the operators \mathcal{P} and \mathcal{Q} are independent of the position \mathbf{x} . We will use this assumption to simplify the notations, but it is straightforward to extend the present framework to cases where the surface properties vary with position along the surface.

If the operator \mathcal{Q} is invertible it is possible to write the surface traction explicitly in terms of the velocity:

$$\mathbf{t}(t) = \mathcal{Z}[\mathbf{u}, \mathbf{n}](t), \quad (2)$$

where \mathcal{Z} is the impedance operator. Alternatively, if \mathcal{P} is invertible, it is possible to write the fluid velocity in terms of the surface traction:

$$\mathbf{u}(t) = \mathcal{Y}[\mathbf{t}, \mathbf{n}](t), \quad (3)$$

in which \mathcal{Y} is the admittance operator.

If we assume that the impedance and admittance operators are linear, continuous and time invariant they can be written as convolution operators [2]:

$$\mathbf{t}(t) = \int_{-\infty}^{+\infty} \mathbf{Z}(\tau) \mathbf{u}(t - \tau) d\tau, \quad \mathbf{u}(t) = \int_{-\infty}^{+\infty} \mathbf{Y}(\tau) \mathbf{t}(t - \tau) d\tau, \quad (4)$$

where \mathbf{Z} and \mathbf{Y} are **the time-domain impedance and admittance functions**. These are square matrices.

In addition to this generalised definition of the impedance boundary condition, one has to specify a boundary condition for temperature. The usual adiabatic or isothermal conditions can be used for this purpose.

2.2. Frequency domain

It is useful to move to the frequency domain by introducing the Fourier transform and its inverse:

$$\hat{f}(\omega) = \int_{-\infty}^{+\infty} f(t) e^{-i\omega t} dt, \quad f(t) = \frac{1}{2\pi} \int_C \hat{f}(\omega) e^{+i\omega t} d\omega, \quad (5)$$

where C is the integration contour for the inverse Fourier transform, which remains to be defined. Quantities expressed in the frequency domain are denoted with a hat.

The convolution operators in Equation (4) relating surface traction and velocity in the time domain become simple multiplications in the frequency domain:

$$\hat{\mathbf{t}}(\omega) = \hat{\mathbf{Z}}(\omega) \hat{\mathbf{u}}(\omega), \quad \hat{\mathbf{u}}(\omega) = \hat{\mathbf{Y}}(\omega) \hat{\mathbf{t}}(\omega). \quad (6)$$

If both the impedance and the admittance operators are defined, then the associated transfer functions are related by $\hat{\mathbf{Z}} = \hat{\mathbf{Y}}^{-1}$.

3. Admissible impedance

A number of constraints can be imposed on the impedance and admittance matrices in order to satisfy basic physical requirements. This section discusses the reality, causality, stability and passivity of the generalised surface impedance.

3.1. Reality

The impedance and admittance functions $\mathbf{Z}(t)$ and $\mathbf{Y}(t)$ should be real valued. It follows that $\hat{\mathbf{Z}}(-\omega^*) = \hat{\mathbf{Z}}(\omega)^*$ and $\hat{\mathbf{Y}}(-\omega^*) = \hat{\mathbf{Y}}(\omega)^*$, in which $*$ denotes the complex conjugate. As a consequence, if an entry of $\hat{\mathbf{Z}}$ or $\hat{\mathbf{Y}}$ has a pole at ω then there should be a matching pole at $-\omega^*$ and the residues for these two poles should be complex conjugates. Additionally if an entry of $\hat{\mathbf{Z}}$ or $\hat{\mathbf{Y}}$ has a zero at ω then there is a matching zero at $-\omega^*$. Note that, if square roots are involved in $\hat{\mathbf{Z}}$ and $\hat{\mathbf{Y}}$, then the associated branch cuts should be chosen carefully.

3.2. Causality

The impedance and admittance functions should be causal, i.e. $\mathbf{Z}(t)$ and $\mathbf{Y}(t)$ should be identically zero for $t < 0$. This implies that the integration contour C in the inverse Fourier transform (5) should be placed below all the poles of the entries of the matrices $\hat{\mathbf{Z}}(\omega)$ and $\hat{\mathbf{Y}}(\omega)$. For $t > 0$, the contour C is closed above so that all the poles are contained within it. For $t < 0$, the contour is closed below and doesn't contain any pole.

3.3. Stability

Causality does not preclude the presence of instabilities since it is possible to have a causal and exponentially growing impedance and admittance functions (provided that the growth rate remains finite). This is the case if there is a pole in the lower half ω plane and the integration contour C is placed below this pole.

The impedance is stable when all the poles of $\hat{\mathbf{Z}}(\omega)$ are in the upper ω plane or on the real axis. The function $\hat{\mathbf{Z}}(\omega)$ is therefore analytic in the lower complex half plane. In this case the integration contour C can be placed infinitely close to the real axis from below. The impedance function then satisfies the Kramers–Kronig relations [11, Section 4.3]:

$$\operatorname{Re}[\mathbf{Z}(\omega)] = \frac{1}{\pi} \oint_{-\infty}^{+\infty} \frac{\operatorname{Im}[\mathbf{Z}(\omega')]}{\omega - \omega'} d\omega', \quad \operatorname{Im}[\mathbf{Z}(\omega)] = \frac{-1}{\pi} \oint_{-\infty}^{+\infty} \frac{\operatorname{Re}[\mathbf{Z}(\omega')]}{\omega - \omega'} d\omega', \quad (7)$$

in which the integrals are to be understood as Cauchy principal values.

If the admittance is stable then all the poles of $\hat{\mathbf{Y}}(\omega)$ are in the upper ω plane or on the real axis. Similar relations to equation (7) hold for the admittance function $\hat{\mathbf{Y}}(\omega)$.

3.4. Passivity

The rate of work per unit area done by the surface traction is given by

$$W = \mathbf{t} \cdot \mathbf{u} = -\mathbf{u} \cdot \boldsymbol{\sigma} \cdot \mathbf{n} = p\mathbf{u} \cdot \mathbf{n} - \mathbf{u} \cdot \boldsymbol{\tau} \cdot \mathbf{n}.$$

This corresponds to the flux of power into the surface due to the mechanical work done by the fluid on the surface. A passive surface receives more energy than it provides to the fluid. At any time T , the net amount of energy into the surface should therefore be non-negative:

$$\int_{-\infty}^T W(t) dt \geq 0, \quad \forall T. \quad (8)$$

The requirement of passivity implies the stability of the surface impedance. If the response function \mathbf{Z} or \mathbf{Y} grows exponentially then the condition above cannot be satisfied for all T and the surface can therefore not be passive.

In the frequency domain, the corresponding quantity is the normal intensity I . Following Fahy [12] we introduce the complex-valued intensity, which, in the present case, takes the form

$$I = \frac{1}{2} \hat{\mathbf{u}}^T \hat{\mathbf{t}}, \quad (9)$$

in which T denotes the Hermitian transpose (i.e. transpose *and* complex conjugation). The real part of I corresponds to the active part of the intensity, i.e. the usual time-averaged energy flux. Conversely, the imaginary part corresponds to the reactive part of the intensity vector. The reactive intensity corresponds to the unsteady energy flow that averages to a zero net flux over a period of oscillation. For more information on the interpretation of the reactive part of the intensity, the reader is referred to Fahy [12] and Bruneau [13].

The frequency-dependent impedance and admittance matrices $\hat{\mathbf{Z}}$ and $\hat{\mathbf{Y}}$ are complex-valued but not necessarily symmetric nor Hermitian. However, these two matrices can be uniquely split between an Hermitian part and a skew-Hermitian part using the Toeplitz decomposition [14]:

$$\hat{\mathbf{Z}} = \hat{\mathbf{R}} + i\hat{\mathbf{X}}, \quad \text{with } \hat{\mathbf{R}} = \frac{1}{2}(\hat{\mathbf{Z}} + \hat{\mathbf{Z}}^T) \quad \text{and } \hat{\mathbf{X}} = \frac{1}{2i}(\hat{\mathbf{Z}} - \hat{\mathbf{Z}}^T), \quad (10)$$

$$\hat{\mathbf{Y}} = \hat{\mathbf{G}} + i\hat{\mathbf{B}}, \quad \text{with } \hat{\mathbf{G}} = \frac{1}{2}(\hat{\mathbf{Y}} + \hat{\mathbf{Y}}^T) \quad \text{and } \hat{\mathbf{B}} = \frac{1}{2i}(\hat{\mathbf{Y}} - \hat{\mathbf{Y}}^T). \quad (11)$$

The matrices $\hat{\mathbf{R}}$, $\hat{\mathbf{X}}$, $\hat{\mathbf{G}}$ and $\hat{\mathbf{B}}$ are Hermitian (hence $i\hat{\mathbf{X}}$ and $i\hat{\mathbf{B}}$ are skew-Hermitian). The Toeplitz decomposition can be understood as the extension to complex matrices of the separation between real and imaginary parts of complex numbers [14]. Therefore, the matrices $\hat{\mathbf{R}}$ and $\hat{\mathbf{X}}$ can be interpreted as generalised definitions of the resistance and the reactance of the surface, respectively. Similarly, $\hat{\mathbf{G}}$ and $\hat{\mathbf{B}}$ provide generalised definitions of the conductance and susceptance.

Using the relation $\hat{\mathbf{t}} = \hat{\mathbf{Z}}\hat{\mathbf{u}}$ together with the splitting of the impedance matrix in terms of resistance and reactance in equation (10), we get the following expression for the complex intensity:

$$I = \frac{1}{2}\hat{\mathbf{u}}^T \hat{\mathbf{R}} \hat{\mathbf{u}} + \frac{i}{2}\hat{\mathbf{u}}^T \hat{\mathbf{X}} \hat{\mathbf{u}}. \quad (12)$$

Since $\hat{\mathbf{R}}$ and $\hat{\mathbf{X}}$ are Hermitian, the quadratic forms $\hat{\mathbf{u}}^T \hat{\mathbf{R}} \hat{\mathbf{u}}$ and $\hat{\mathbf{u}}^T \hat{\mathbf{X}} \hat{\mathbf{u}}$ are real. The first term (resp. second term) in this expression is real valued (resp. purely imaginary) and therefore corresponds to the active intensity (resp. reactive intensity). This shows that the Toeplitz decomposition (10) leads directly to the separation of the active and reactive parts of the intensity. Instead if we use the relation $\hat{\mathbf{u}} = \hat{\mathbf{Y}}\hat{\mathbf{t}}$ and equation (11) we get

$$I = \frac{1}{2}\hat{\mathbf{t}}^T \hat{\mathbf{G}} \hat{\mathbf{t}} - \frac{i}{2}\hat{\mathbf{t}}^T \hat{\mathbf{B}} \hat{\mathbf{t}}. \quad (13)$$

Again we can identify the first term (real valued) as the active intensity and the second term (purely imaginary) as the reactive intensity.

To have a passive surface, the time-average flux of energy should be non-negative, i.e. $\text{Re}(I) \geq 0$. This implies that we should have $\hat{\mathbf{u}}^T \hat{\mathbf{R}} \hat{\mathbf{u}} \geq 0$ for any $\hat{\mathbf{u}}$, as well as $\hat{\mathbf{t}}^T \hat{\mathbf{G}} \hat{\mathbf{t}} \geq 0$ for any $\hat{\mathbf{t}}$. The resistance matrix $\hat{\mathbf{R}}$ and the conductance matrix $\hat{\mathbf{G}}$ should therefore be positive semidefinite. In other words the matrices $\hat{\mathbf{Z}}$ and $\hat{\mathbf{Y}}$ should have positive semidefinite Hermitian parts. It is useful to recall the result from Mathias [15]: if a complex square matrix has a positive definite Hermitian part, then its inverse also has a positive definite Hermitian part. Therefore if $\hat{\mathbf{R}}$ is positive definite, then $\hat{\mathbf{G}}$ is also positive definite (the reverse is also true).

If the resistance matrix $\hat{\mathbf{R}}$ is positive semidefinite then we have the following results, obtained using Corollary 7.1.5 from Horn & Johnson [14]:

$$\hat{R}_{ii} \geq 0, \quad \forall i, \quad \text{and } |\hat{R}_{ij}| \leq \sqrt{\hat{R}_{ii}\hat{R}_{jj}}, \quad \forall i, j \text{ with } i \neq j. \quad (14)$$

Similar properties hold for $\hat{\mathbf{G}}$. As a consequence we have the following results for a passive surface:

$$\text{Re}(\hat{Z}_{ii}) \geq 0, \quad \forall i, \quad \text{and } |\hat{Z}_{ij} + \hat{Z}_{ji}^*| \leq 2\sqrt{\text{Re}(\hat{Z}_{ii})\text{Re}(\hat{Z}_{jj})}, \quad \forall i, j \text{ with } i \neq j, \quad (15)$$

$$\text{Re}(\hat{Y}_{ii}) \geq 0, \quad \forall i, \quad \text{and } |\hat{Y}_{ij} + \hat{Y}_{ji}^*| \leq 2\sqrt{\text{Re}(\hat{Y}_{ii})\text{Re}(\hat{Y}_{jj})}, \quad \forall i, j \text{ with } i \neq j. \quad (16)$$

The diagonal terms in $\hat{\mathbf{Z}}$ and $\hat{\mathbf{Y}}$ have non-negative real parts. In addition the magnitudes of $\hat{Z}_{ij} + \hat{Z}_{ji}^*$ and $\hat{Y}_{ij} + \hat{Y}_{ji}^*$ should be bounded. This is the main result of the present paper. It provides a generalisation of the requirement that the classical, scalar impedance has a real part.

It is worth noting that the property that $\hat{\mathbf{R}}$ and $\hat{\mathbf{G}}$ are positive semidefinite for a passive surface applies irrespective of the coordinate system used to define the entries of these matrices. In other words, the properties in equations (15) and (16) apply in any orthonormal coordinate system. This is shown by introducing the unitary matrix \mathbf{U} corresponding to a rotation of the coordinate system. The fluid velocity and the surface traction represented in this new coordinate system are denoted by $\tilde{\mathbf{u}} = \mathbf{U}\mathbf{\hat{u}}$ and $\tilde{\mathbf{t}} = \mathbf{U}\mathbf{\hat{t}}$. The definitions of the impedance and admittance relations become $\tilde{\mathbf{t}} = \tilde{\mathbf{Z}}\tilde{\mathbf{u}}$ and $\tilde{\mathbf{u}} = \tilde{\mathbf{Y}}\tilde{\mathbf{t}}$, in which $\tilde{\mathbf{Z}} = \mathbf{U}\hat{\mathbf{Z}}\mathbf{U}^T$ and $\tilde{\mathbf{Y}} = \mathbf{U}\hat{\mathbf{Y}}\mathbf{U}^T$. It is straightforward to show that the Hermitian parts of $\tilde{\mathbf{Z}}$ and $\tilde{\mathbf{Y}}$ are also positive semidefinite, see Observation 7.1.8 in [14].

Since the resistance matrix is Hermitian, it can be diagonalised as $\hat{\mathbf{R}} = \hat{\mathbf{Q}}\hat{\Lambda}\hat{\mathbf{Q}}^T$ where $\hat{\mathbf{Q}}$ is a unitary matrix and $\hat{\Lambda}$ is a diagonal matrix of real-valued eigenvalues. As a result we have the following expression for the active intensity:

$$\text{Re}(I) = \sum_n \lambda_n |\tilde{u}_n|^2, \quad (17)$$

where we have introduced $\tilde{\mathbf{u}} = \hat{\mathbf{Q}}\mathbf{\hat{u}}$ which corresponds to a change of coordinate system associated with the unitary matrix $\hat{\mathbf{Q}}$. For a passive surface the eigenvalues λ_n are non-negative. A similar result can be obtained for the conductance matrix $\hat{\mathbf{G}}$.

4. Two-dimensional case

To illustrate the proposed formulation, we can consider the two-dimensional case by writing

$$\begin{pmatrix} \hat{t}_n \\ \hat{t}_t \end{pmatrix} = \begin{bmatrix} \hat{Z}_{nn} & \hat{Z}_{nt} \\ \hat{Z}_{tn} & \hat{Z}_{tt} \end{bmatrix} \begin{pmatrix} \hat{u}_n \\ \hat{u}_t \end{pmatrix}, \quad \text{and} \quad \begin{pmatrix} \hat{t}_n \\ \hat{t}_t \end{pmatrix} = \begin{pmatrix} \hat{p} - \hat{\tau}_{nn} \\ -\hat{\tau}_{nt} \end{pmatrix}, \quad (18)$$

where the subscripts n and t denote the normal and tangential components, respectively.

While the term \hat{Z}_{nn} is related to the traditional acoustic impedance, the term \hat{Z}_{tt} represents the friction generated when the fluid elements slide along the surface. The momentum transfer impedance considered by Schultz *et al* [8] is represented by the cross term \hat{Z}_{tn} which describes the tangential force generated by a normal velocity. Conversely, the term \hat{Z}_{nt} describes the normal force generated by a tangential velocity. The friction coefficient considered by Aurégan [9] is represented by \hat{Z}_{tt} which relates the tangential velocity and the tangential surface traction. It is expected that the cross terms \hat{Z}_{nt} and \hat{Z}_{tn} will be involved for instance in a perforated plate where the holes are drilled at an angle from the normal to the plate.

As indicated above, the resistance matrix of a passive surface should be positive semidefinite and it follows that

$$\text{Re}(\hat{Z}_{nn}) \geq 0, \quad \text{Re}(\hat{Z}_{tt}) \geq 0, \quad |\hat{Z}_{tn} + \hat{Z}_{nt}^*| \leq 2\sqrt{\text{Re}(\hat{Z}_{nn})\text{Re}(\hat{Z}_{tt})}. \quad (19)$$

We therefore recover the traditional condition on the real part of the classical impedance \hat{Z}_{nn} . A similar constraint applies for the tangential component \hat{Z}_{tt} . We have also an inequality satisfied by the off-diagonal terms of the impedance matrix. This indicates that if either \hat{Z}_{nn} or \hat{Z}_{tt} is purely imaginary (for instance for a purely reactive acoustic treatment) then $\hat{Z}_{tn} = -\hat{Z}_{nt}^*$.

The standard impedance condition is recovered by neglecting viscosity and setting $\hat{Z}_{nt} = \hat{Z}_{tn} = \hat{Z}_{tt} = 0$. In this case we have $\hat{p} = \hat{Z}_{nn}\hat{u}_n$. Note however that it is not always possible to define the impedance and admittance matrices. In this case it is preferable to use the more general framework of equation (1). An example is when the normal velocity is set to zero and the slip condition (zero tangential force) is applied. This can be written

$$\begin{bmatrix} 0 & 0 \\ 0 & 1 \end{bmatrix} \begin{pmatrix} t_n \\ t_t \end{pmatrix} = \begin{bmatrix} 1 & 0 \\ 0 & 0 \end{bmatrix} \begin{pmatrix} u_n \\ u_t \end{pmatrix}. \quad (20)$$

In this particular case it is not possible to define the impedance matrix nor the admittance matrix.

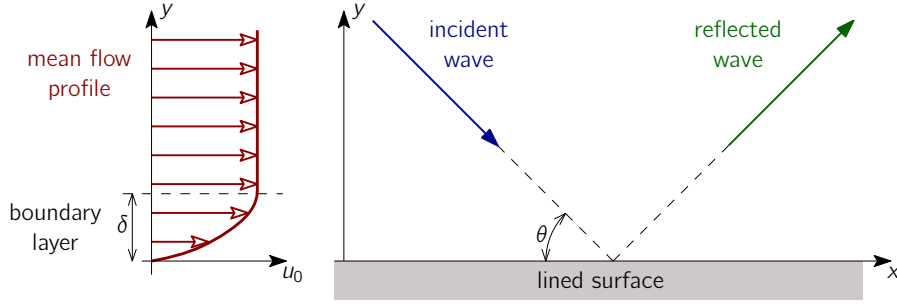


Figure 1: Diagram of a plane wave reflected by a flat surface in the presence of a grazing mean flow.

5. Example

To illustrate the impact of the generalised impedance condition, we consider the reflection of an acoustic plane wave off a flat surface where the generalised impedance condition is imposed, see Figure 1.

5.1. Numerical model

The problem is two-dimensional with the surface defined by $y = 0$ and the waves propagating in the region $y > 0$. The incident acoustic plane wave has an angular frequency ω and an angle of incidence θ . There is a mean flow over the surface. The boundary layer of the mean flow is confined to the region $0 < y < \delta$ where δ is the boundary layer thickness. Above the boundary layer ($y > \delta$) the mean flow is uniform with velocity U_0 along the x axis. In the boundary layer we have a parallel shear flow along the x axis, with a velocity profile denoted by $u_0(y)$. The mean density ρ_0 and sound speed c_0 are considered uniform. The fluid is viscous and heat conductive, with shear viscosity μ , bulk viscosity μ_b and heat conductivity κ .

The linear propagation of small perturbations of the mean flow is governed by the linearised Navier–Stokes equations (linearised conservation of mass, momentum and total energy). In two dimensions these are written as follows

$$\frac{\partial}{\partial t}(\mathbf{M}\mathbf{q}) + \frac{\partial}{\partial x} \left(\mathbf{F}_x \mathbf{q} - \mathbf{G}_{xx} \frac{\partial \mathbf{q}}{\partial x} - \mathbf{G}_{xy} \frac{\partial \mathbf{q}}{\partial y} \right) + \frac{\partial}{\partial y} \left(\mathbf{F}_y \mathbf{q} - \mathbf{G}_{yx} \frac{\partial \mathbf{q}}{\partial x} - \mathbf{G}_{yy} \frac{\partial \mathbf{q}}{\partial y} \right) = \mathbf{0}, \quad (21)$$

where the vector of field variables $\mathbf{q} = (\rho', u'_x, u'_y, T')$ contains the perturbations of density, velocity and temperature. The coefficient matrices \mathbf{M} , \mathbf{F}_x , \mathbf{F}_y , \mathbf{G}_{xx} , \mathbf{G}_{xy} , \mathbf{G}_{yx} and \mathbf{G}_{yy} are given in Appendix A. Since we consider a parallel shear flow, these matrices depend only on the transverse coordinate y .

Above the boundary layer ($y > \delta$), the incoming acoustic wave is written

$$\mathbf{q}^-(x, y, t) = \hat{\mathbf{q}}^- \exp\{i\omega t - ik_x x - ik_y^- y\},$$

with the wavenumbers $k_x = k^- \cos(\theta)$ and $k_y^- = -k^- \sin(\theta)$. The vector $\hat{\mathbf{q}}^-$ and the wavenumber k^- are solutions of the dispersion relation associated with equation (21). Appendix B details the numerical solution of this dispersion relation.

Fourier transforms are applied in time and the x coordinate, which is equivalent to seeking solutions of the form

$$\mathbf{q}(x, y, t) = \hat{\mathbf{q}}(y) \exp\{i\omega t - ik_x x\}.$$

Since the coefficient matrices are independent of x the governing equations become

$$i\omega \mathbf{M} \hat{\mathbf{q}} - ik_x \left(\mathbf{F}_x \hat{\mathbf{q}} + ik_x \mathbf{G}_{xx} \hat{\mathbf{q}} - \mathbf{G}_{xy} \frac{d\hat{\mathbf{q}}}{dy} \right) + \frac{d}{dy} \left(\mathbf{F}_y \hat{\mathbf{q}} + ik_x \mathbf{G}_{yx} \hat{\mathbf{q}} - \mathbf{G}_{yy} \frac{d\hat{\mathbf{q}}}{dy} \right) = \mathbf{0}. \quad (22)$$

On the surface $y = 0$ the generalised impedance condition (6) is applied, together with the adiabatic boundary condition $dT'/dy = 0$ for the temperature.

On the upper boundary of the computational domain, $y = H$, the solution \mathbf{q} is written as the sum of the incident acoustic wave with angle θ and a combination of reflected waves:

$$\mathbf{q}(x, y, t) = \left(\hat{\mathbf{q}}^- \exp\{-ik_y^- y\} + \sum_{n=1}^3 \hat{A}_n \hat{\mathbf{q}}_n^+ \exp\{-ik_{yn}^+ y\} \right) \exp\{i\omega t - ik_x x\}, \quad \text{for } y > \delta, \quad (23)$$

where \hat{A}_n represent the unknown amplitudes of the reflected waves. Appendix C explains how the wavenumbers k_{yn}^+ and vectors $\hat{\mathbf{q}}_n^+$ are obtained from the dispersion relation of the linearised Navier–Stokes equations.

The one-dimensional governing equations, together with the boundary conditions, are solved using a spectral Galerkin method. The details of the implementation are given in Appendix D.

5.2. Results without mean flow

We first consider the case without mean flow by setting $u_0 = 0$. The fluid is air whose properties are $\rho_0 = 1.2 \text{ kg/m}^3$, $T_0 = 293 \text{ K}$, $c_p = 1012 \text{ J/K/kg}$, $\gamma = 1.4$, $\mu = 1.85 \cdot 10^{-5} \text{ kg/m/s}$ and $\kappa = 0.026 \text{ W/m/K}$. The incident plane wave has a frequency of 1 kHz. We vary its angle of incidence θ and calculate the reflection coefficient of the acoustic wave. For reference, with these parameters, the thickness of the unsteady viscous boundary layer is $\delta_v = 70 \mu\text{m}$ and the thickness of the unsteady thermal boundary layer is $\delta_t = 83 \mu\text{m}$. Comparatively, the acoustic wavelength is approximately 344 mm.

Figure 2a shows the magnitude of this coefficient as a function of θ , for $\hat{Z}_{nn} = (5 - i)\rho_0 c_0$, $\hat{Z}_{nn} = \hat{Z}_{nt} = 0$ and for various values of \hat{Z}_{tt} . We therefore have a fixed standard impedance and vary the friction coefficient of the surface. It is clear that in this case the friction coefficient has a negligible effect on the acoustic wave (there is however an effect on the amplitude of the vorticity wave present in the vicinity of the surface $y = 0$). Also shown in Figure 2a is the reflection coefficient obtained with the standard impedance condition (i.e. for an inviscid model). All the results shown in this graph are identical to those obtained with the standard impedance.

Figure 2b shows the results when $\hat{Z}_{nn} = -\hat{Z}_{nt} = \rho_0 c_0 / 10$. In this case the friction coefficient has a significant impact on the acoustic attenuation by the surface. When the friction coefficient is large, one recovers the solution in Figure 2a. It is interesting to note that when the off-diagonal terms of the impedance matrix are non-zero, there is an asymmetry in the reflection coefficient (i.e. between $\theta < 90^\circ$ and $\theta > 90^\circ$). It can be seen that the results with the generalised impedance differ significantly from that obtained with the standard impedance condition.

If we now fix both $\hat{Z}_{nn} = (5 - i)\rho_0 c_0$ and $\hat{Z}_{tt} = 0$ and vary $\hat{Z}_{nn} = -\hat{Z}_{nt}$ we get the results in Figure 3a. Increasing \hat{Z}_{nn} results in a significant increase of the reflection coefficient for most incidence angles. When the friction coefficient is set to a non-zero value $\hat{Z}_{tt} = 0.005\rho_0 c_0$, we can see in Figure 3b that the cross terms \hat{Z}_{nn} and \hat{Z}_{nt} have a more limited impact on the reflection coefficient.

5.3. Results with flow

We use a sine function to describe the velocity profile inside the boundary layer:

$$u_0(y) = \begin{cases} M c_0 \sin\left(\frac{\pi y}{2\delta}\right) & \text{for } 0 < y < \delta \\ M c_0 & \text{for } y > \delta \end{cases}.$$

The Mach number is $M = 0.5$. Other profiles have been considered (polynomial profiles from linear to quintic). And the same trends as those discussed below have been observed.

Results are presented in Figures 4 and 5 and the trends are similar to those observed for the no flow case. When $\hat{Z}_{nn} = \hat{Z}_{nt} = 0$ varying \hat{Z}_{tt} has very little influence on the reflection coefficient (see Figure 4a). However, when the cross terms are non-zero, with $\hat{Z}_{nn} = \hat{Z}_{nt} = \rho_0 c_0 / 10$ in this case, the friction coefficient \hat{Z}_{tt} has a significant impact on the reflection coefficient (see Figure 4b). The overall trend is that the reflection coefficient increases when \hat{Z}_{tt} increases. Again these results match closely those obtained with the standard definition of the impedance.

Similarly to the no-flow case, varying the cross terms \hat{Z}_{nn} and \hat{Z}_{nt} leads to large variations of the reflection coefficient, see Figure 5. These variations are more significant when the friction coefficient \hat{Z}_{tt} is small. In this case, there is a significant difference between the results of the generalised impedance and those of the standard impedance.

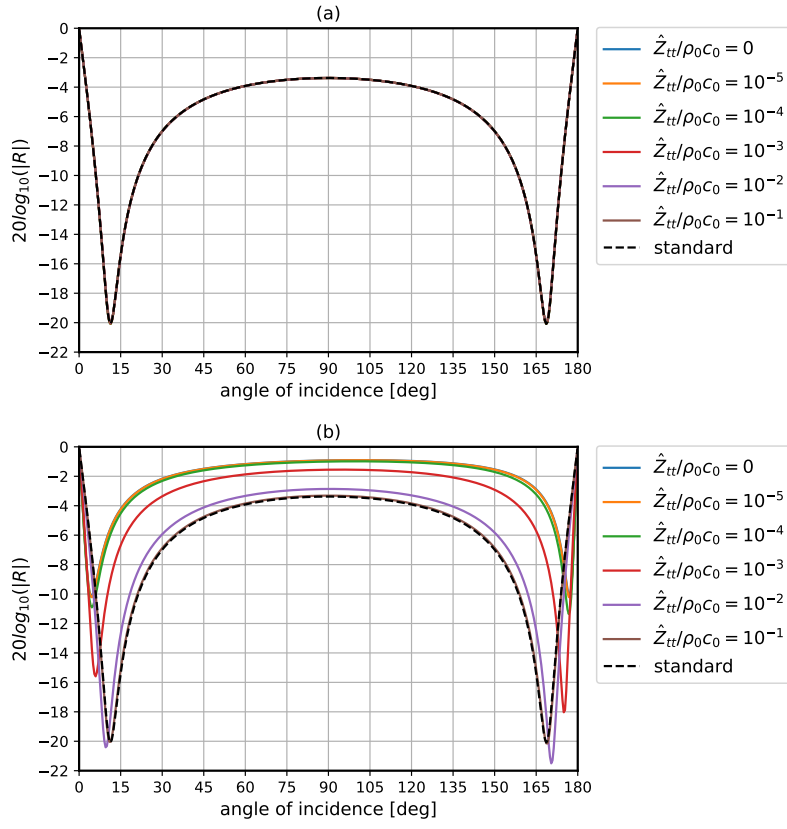


Figure 2: Reflection coefficient without mean flow as a function of θ , for $\hat{Z}_{tn} = (5 - i)\rho_0 c_0$ and for various values of \hat{Z}_{tt} . (a) $\hat{Z}_{tn} = \hat{Z}_{nt} = 0$; (b) $\hat{Z}_{tn} = -\hat{Z}_{nt} = \rho_0 c_0 / 10$.

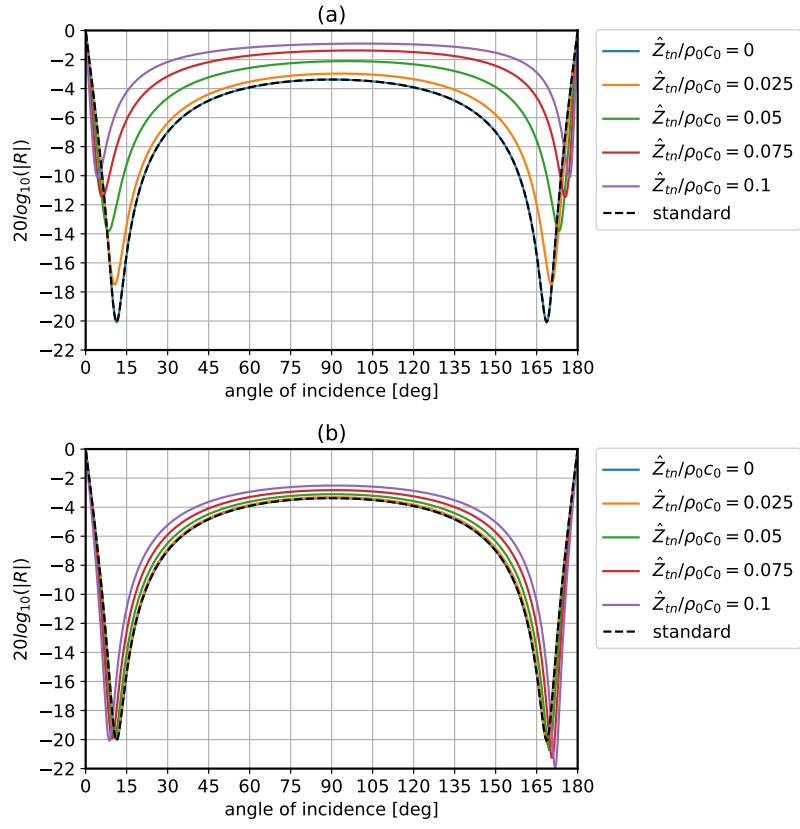


Figure 3: Reflection coefficient without mean flow as a function of θ , for $\hat{Z}_{nm} = (5 - i)\rho_0 c_0$ and for various values of $\hat{Z}_{tn} = -\hat{Z}_{mt}$. (a) $\hat{Z}_{tt} = 0$; (b) $\hat{Z}_{tt}/\rho_0 c_0 = 0.005$.

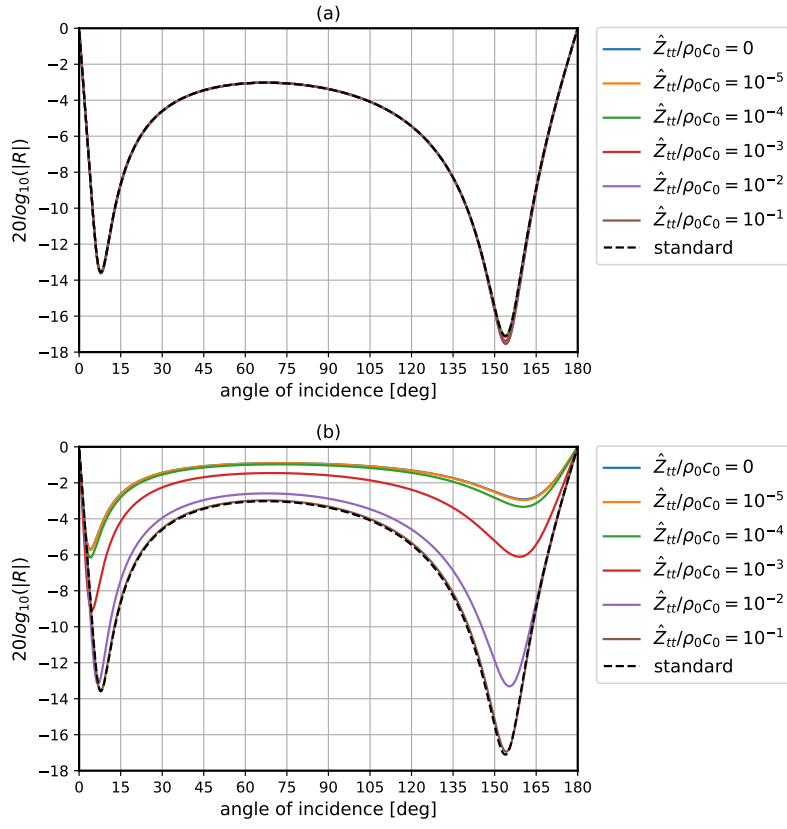


Figure 4: Reflection coefficient with mean flow as a function of θ , for $\hat{Z}_{tm} = (5 - i)\rho_0 c_0$ and for various values of \hat{Z}_{tt} . (a) $\hat{Z}_{tm} = \hat{Z}_{nt} = 0$; (b) $\hat{Z}_{tm} = -\hat{Z}_{nt} = \rho_0 c_0 / 10$.

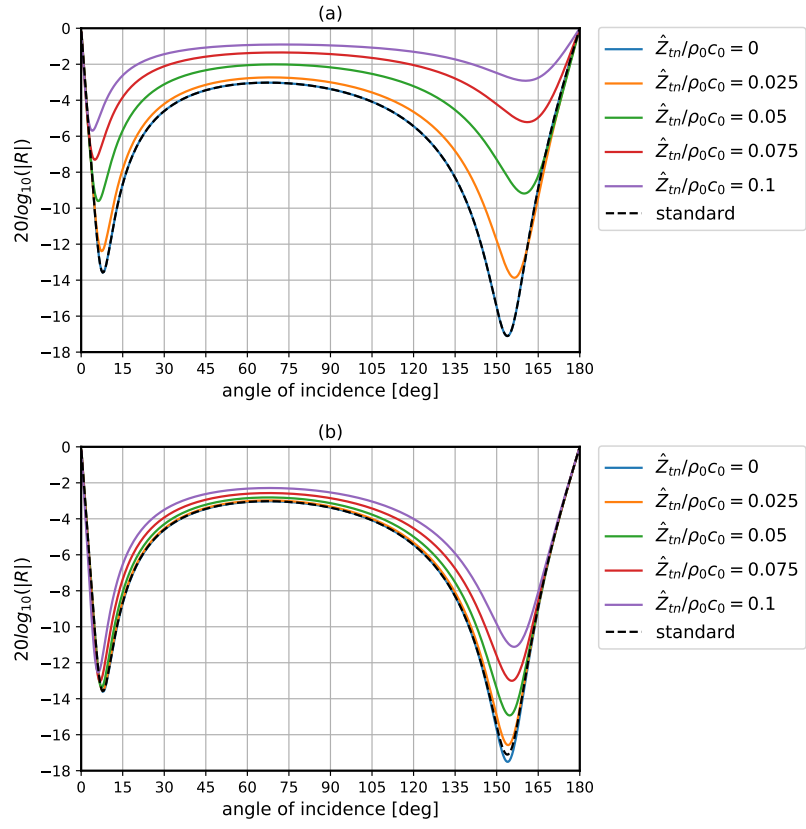


Figure 5: Reflection coefficient with mean flow as a function of θ , for $\hat{Z}_{nn} = (5 - i)\rho_0 c_0$ and for various values of $\hat{Z}_{tn} = -\hat{Z}_{nt}$. (a) $\hat{Z}_{tt} = 0$; (b) $\hat{Z}_{tt}/\rho_0 c_0 = 0.005$.

6. Summary and perspectives

We have considered a generalised definition of the acoustic impedance where a linear dependence is assumed between the fluid velocity and the force on the surface. It is possible to define admissibility conditions such as the reality, causality, stability and passivity of the surface. This last condition leads to a generalisation of the requirement that the resistance should be positive. The reflection of a plane wave by a lined surface was then used as a way to illustrate the influence of the additional parameters introduced by the generalised impedance. It was found that the cross terms \hat{Z}_{nt} and \hat{Z}_{tn} and the friction coefficient \hat{Z}_{tt} can have a significant influence on the reflection coefficient.

The present paper provides the theoretical framework for a generalised definition of the impedance. Experimental investigations will be necessary to attempt to measure the admittance or impedance matrix. The questions to address are (i) how one can measure these matrices and (ii) to what extent are these effects significant in practical cases.

A number of models are available to describe the classical impedance of acoustic treatments, in particular perforated liners, for instance [16] and [17]. How the additional terms \hat{Z}_{tt} , \hat{Z}_{nt} and \hat{Z}_{tn} could be modelled remains to be investigated. A possible approach would be to use homogenisation methods such as those developed in [18] and [19].

Finally detailed computational modelling (using direct numerical simulations or large eddy simulations) would be useful to study the impact of the generalised impedance on the acoustic field and the grazing flow.

Appendix A. Coefficient matrices

The coefficient matrices that appear in the linearised Navier–Stokes equations (21) are defined as follows:

$$\mathbf{M} = \begin{bmatrix} 1 & 0 & 0 & 0 \\ u_0 & \rho_0 & 0 & 0 \\ 0 & 0 & \rho_0 & 0 \\ e_0 & \rho_0 u_0 & 0 & \rho_0 C_v \end{bmatrix}, \quad (\text{A.1})$$

$$\mathbf{F}_x = \begin{bmatrix} u_0 & \rho_0 & 0 & 0 \\ u_0^2 + RT_0 & 2\rho_0 u_0 & 0 & \rho_0 R \\ 0 & 0 & \rho_0 u_0 & 0 \\ (e_0 + RT_0)u_0 & \rho_0 e_0 + p_0 + \rho_0 u_0^2 & -\mu u_0' & p_0 + \rho_0 u_0 C_p \end{bmatrix}, \quad \mathbf{F}_y = \begin{bmatrix} 0 & 0 & \rho_0 & 0 \\ 0 & 0 & \rho_0 u_0 & 0 \\ RT_0 & 0 & 0 & \rho_0 R \\ 0 & -\mu u_0' & p_0 + \rho_0 e_0 & 0 \end{bmatrix}, \quad (\text{A.2})$$

$$\mathbf{G}_{xx} = \begin{bmatrix} 0 & 0 & 0 & 0 \\ 0 & 0 & \mu_b + \frac{4}{3}\mu & 0 \\ 0 & 0 & \mu & 0 \\ 0 & 0 & (\mu_b + \frac{4}{3}\mu)u_0 & \kappa \end{bmatrix}, \quad \mathbf{G}_{xy} = \begin{bmatrix} 0 & 0 & 0 & 0 \\ 0 & 0 & \mu_b - \frac{2}{3}\mu & 0 \\ 0 & \mu & 0 & 0 \\ 0 & 0 & (\mu_b - \frac{2}{3}\mu)u_0 & 0 \end{bmatrix}, \quad (\text{A.3})$$

$$\mathbf{G}_{yx} = \begin{bmatrix} 0 & 0 & 0 & 0 \\ 0 & 0 & \mu & 0 \\ 0 & \mu_b - \frac{2}{3}\mu & 0 & 0 \\ 0 & 0 & \mu u_0 & 0 \end{bmatrix}, \quad \mathbf{G}_{yy} = \begin{bmatrix} 0 & 0 & 0 & 0 \\ 0 & \mu & 0 & 0 \\ 0 & 0 & \mu_b + \frac{4}{3}\mu & 0 \\ 0 & \mu u_0 & 0 & \kappa \end{bmatrix}, \quad (\text{A.4})$$

in which C_p and C_v are the heat capacity of the fluid, at constant pressure and volume, respectively. We have also introduced $R = C_p - C_v$ and $e_0 = C_v T_0 + u_0^2/2$.

Appendix B. Dispersion relation

The dispersion relation of the linearised Navier–Stokes equations (21) is obtained by seeking plane wave solutions of the form:

$$\mathbf{q}(x, y, t) = \tilde{\mathbf{q}} \exp\{i\omega t - ikx \cos \theta - iky \sin \theta\},$$

in which k is the wavenumber and θ the plane wave direction. Introducing this ansatz in Equation (21) yields the dispersion relation

$$(i\omega \mathbf{M} - ik\mathbf{A} - k^2 \mathbf{B})\tilde{\mathbf{q}} = \mathbf{0},$$

with

$$\mathbf{A} = \mathbf{F}_x \cos \theta + \mathbf{F}_y \sin \theta, \quad \text{and} \quad \mathbf{B} = \mathbf{G}_{xx} \cos^2 \theta + \mathbf{G}_{yy} \sin^2 \theta + (\mathbf{G}_{xy} + \mathbf{G}_{yx}) \cos \theta \sin \theta.$$

For a given angle θ , the dispersion relation is a quadratic eigenvalue problem for the wavenumber k (with eigenvector $\tilde{\mathbf{q}}$). This problem can be easily solved numerically to obtain 8 eigenvalue-eigenvector pairs. Three of these have wavenumbers with positive real parts and correspond to the acoustic, vortical and entropy waves propagating in the θ direction. Three other eigenvalues correspond to the waves propagating in the opposite direction. The remaining solutions have zero phase velocity ω/k (to machine precision) and do not correspond to physical waves. The acoustic wave propagating in the θ direction is easily identified as having the phase speed with the largest real part. This provides the value of k^- as well as the corresponding eigenvector $\tilde{\mathbf{q}}^-$ introduced in Section 5.1.

Appendix C. Reflected plane waves

To define the plane waves that are reflected into the uniform mean flow ($y > \delta$) it is also necessary to solve the dispersion relation of the linearised Navier–Stokes equation. Instead of fixing the direction θ , the wavenumber k_x is prescribed by the incident plane wave. We therefore seek solutions of the form

$$\mathbf{q}(x, y, t) = \tilde{\mathbf{q}} \exp\{i\omega t - ik_x x - ik_y y\},$$

in which $k_x = k^- \cos(\theta)$ is fixed. This leads to the following expression

$$(\mathbf{C}_0 - ik_y \mathbf{C}_1 - k_y^2 \mathbf{C}_2) \tilde{\mathbf{q}} = \mathbf{0},$$

with

$$\mathbf{C}_0 = i\omega \mathbf{M} - ik_x \mathbf{F}_x - k_x^2 \mathbf{G}_{xx}, \quad \mathbf{C}_1 = \mathbf{F}_y - ik_x (\mathbf{G}_{xy} + \mathbf{G}_{yx}), \quad \mathbf{C}_2 = \mathbf{G}_{yy}.$$

This represents a quadratic eigenvalue problem for the wavenumber k_y and the associated eigenvector $\tilde{\mathbf{q}}$. Again one finds 8 eigenvalue-eigenvector pairs, three of which correspond to the acoustic, vortical and entropy waves propagating in the positive y direction. The remaining two solutions have zero phase velocity ω/k (to machine precision) and do not correspond to physical waves (they are artefacts of the mathematics). These are the waves that are used to define the wavenumbers k_{yn}^+ and the vectors $\tilde{\mathbf{q}}_n^+$ introduced in Equation (23).

Appendix D. Spectral Galerkin method

The linearised Navier–Stokes equations (22) are solved using a spectral Galerkin method. A variational formulation is obtained by projecting (22) onto a vector \mathbf{w} of test functions and integrating over the computational domain $0 < y < H$. After integration by parts we can write:

$$\int_0^H \left\{ i\omega \mathbf{w}^T \mathbf{M} \hat{\mathbf{q}} - ik_x \mathbf{w}^T \left(\mathbf{F}_x \hat{\mathbf{q}} + ik_x \mathbf{G}_{xx} \hat{\mathbf{q}} - \mathbf{G}_{xy} \frac{d\hat{\mathbf{q}}}{dy} \right) - \frac{d\mathbf{w}^T}{dy} \left(\mathbf{F}_y \hat{\mathbf{q}} + ik_x \mathbf{G}_{yx} \hat{\mathbf{q}} - \mathbf{G}_{yy} \frac{d\hat{\mathbf{q}}}{dy} \right) \right\} dy + \mathbf{w}(H)^T \mathbf{f}(H) - \mathbf{w}(0)^T \mathbf{f}(0) = 0, \quad (\text{D.1})$$

in which

$$\mathbf{f} = \mathbf{F}_y \hat{\mathbf{q}} + ik_x \mathbf{G}_{yx} \hat{\mathbf{q}} - \mathbf{G}_{yy} \frac{d\hat{\mathbf{q}}}{dy}$$

represents the flux of mass, momentum and energy along the y direction. It is precisely these fluxes at $y = 0$ and H that have to be modified to enforce the boundary conditions in the variational formulation.

For the generalised impedance condition at $y = 0$, the surface traction corresponds to the second and third components of the flux vector \mathbf{f} . The natural boundary condition is therefore the impedance condition written in (18) which provides the surface traction in terms of the velocity vector. We can write

$$\begin{pmatrix} \hat{t}_n \\ \hat{t}_t \end{pmatrix} = \begin{bmatrix} 0 & 0 & 1 & 0 \\ 0 & 1 & 0 & 0 \end{bmatrix} \mathbf{f}, \quad \begin{pmatrix} \hat{u}_n \\ \hat{u}_t \end{pmatrix} = \begin{pmatrix} -\hat{u}_y \\ -\hat{u}_x \end{pmatrix} = - \begin{bmatrix} 0 & 0 & 1 & 0 \\ 0 & 1 & 0 & 0 \end{bmatrix} \hat{\mathbf{q}},$$

It follows that the generalised impedance condition can be enforced by replacing $\hat{\mathbf{f}}(0)$ in equation (D.1) by

$$\begin{bmatrix} 1 & 0 & 0 & 0 \\ 0 & 0 & 0 & 0 \\ 0 & 0 & 0 & 0 \\ 0 & 0 & 0 & 1 \end{bmatrix} \mathbf{f}(0) - \begin{bmatrix} 0 & 0 \\ 0 & 1 \\ 1 & 0 \\ 0 & 0 \end{bmatrix} \hat{\mathbf{z}} \begin{bmatrix} 0 & 0 & 1 & 0 \\ 0 & 1 & 0 & 0 \end{bmatrix} \hat{\mathbf{q}}(0).$$

In addition, in the calculation of $\mathbf{f}(0)$ in this last expression, the last entry of the matrix \mathbf{G}_{yy} (which is κ) is set to zero to enforce the adiabatic boundary condition on temperature.

For the radiation condition at the upper boundary $y = H$ the flux term $\hat{f}(H)$ is written in terms of the incoming and reflected waves:

$$\hat{f}(H) = (\mathbf{F}_y + ik_x \mathbf{G}_{yx} + ik_y^- \mathbf{G}_{yy}) \hat{\mathbf{q}}^- \exp\{-ik_y^- H\} + \sum_{n=1}^3 \hat{A}_n (\mathbf{F}_y + ik_x \mathbf{G}_{yx} + ik_{yn}^+ \mathbf{G}_{yy}) \hat{\mathbf{q}}_n^+ \exp\{-ik_{yn}^+ H\} .$$

The first term goes to the right-hand side of the system since this is the forcing term due to the incident wave. The introduction of the wave amplitudes \hat{A}_n requires additional equations to close the problem. This is done by writing equation (23) at $y = H$

$$\hat{\mathbf{q}}(y = H) = \hat{\mathbf{q}}^- \exp\{-ik_y^- H\} + \sum_{n=1}^3 \hat{A}_n \hat{\mathbf{q}}_n^+ \exp\{-ik_{yn}^+ H\} .$$

It was verified *a posteriori* that these two boundary conditions are indeed satisfied by the numerical solutions.

References

- [1] S. Rienstra, Impedance models in time domain, including the extended Helmholtz resonator model, in: 12th AIAA/CEAS Aeroacoustics Conference, Cambridge, MA, USA, 2006, AIAA paper 2006-2686.
- [2] F. Monteghetti, Analysis and discretization of time-domain impedance boundary conditions in aeroacoustics, Ph.D. thesis, ISAE-SUPAERO, Université de Toulouse, Toulouse, France (2018).
URL <https://hal.archives-ouvertes.fr/te1-01910643v1>
- [3] C. Tam, L. Auriault, Time-domain impedance boundary conditions for computational aeroacoustics, AIAA journal 34 (5) (1996) 917–923.
- [4] S. Olivetti, R. Sandberg, B. Tester, Direct numerical simulation of turbulent flow with an impedance condition, Journal of Sound and Vibration 344 (2015) 28–37.
- [5] C. Scalo, J. Bodart, S. Lele, Compressible turbulent channel flow with impedance boundary conditions, Physics of Fluids 27 (3) (2015) 035107.
- [6] R. Sebastian, D. Marx, V. Fortuné, Numerical simulation of a turbulent channel flow with an acoustic liner, Journal of Sound and Vibration 456 (2019) 306–330.
- [7] Y. Renou, Y. Aurégan, Failure of the Ingard–Myers boundary condition for a lined duct: An experimental investigation, Journal of the Acoustical Society of America 130 (1) (2012) 52–60.
- [8] A. Schulz, C. Weng, F. Bake, L. Enghardt, D. Ronneberger, Modeling of liner impedance with grazing shear flow using a new momentum transfer boundary condition, in: 23rd AIAA/CEAS Aeroacoustics Conference, 2017, AIAA paper 2017-3377.
- [9] Y. Aurégan, On the use of a stress–impedance model to describe sound propagation in a lined duct with grazing flow, The Journal of the Acoustical Society of America 143 (5) (2018) 2975–2979. doi:10.1121/1.5037585.
URL <https://doi.org/10.1121/1.5037585>
- [10] X. Dai, Y. Aurégan, Acoustic of a perforated liner with grazing flow: Floquet-bloch periodical approach versus impedance continuous approach, The Journal of the Acoustical Society of America 140 (3) (2016) 2047–2055.
- [11] V. Lucarini, J. Saarinen, K.-E. Peiponen, E. Vartiainen, Kramers–Kronig relations in optical materials research, Vol. 110, Springer Science & Business Media, 2005.
- [12] F. Fahy, Sound Intensity, CRC Press, 2002.
- [13] M. Bruneau, Fundamentals of acoustics, John Wiley & Sons, 2013.
- [14] R. Horn, C. Johnson, Matrix analysis, Cambridge University Press, 2012.
- [15] R. Mathias, Matrices with positive definite Hermitian part: Inequalities and linear systems, SIAM journal on matrix analysis and applications 13 (2) (1992) 640–654.
- [16] A. Guess, Calculation of perforated plate liner parameters from specified acoustic resistance and reactance, Journal of Sound and Vibration 40 (1) (1975) 119–137.
- [17] D.-Y. Maa, Potential of microperforated panel absorber, The Journal of the Acoustical Society of America 104 (5) (1998) 2861–2866.
- [18] E. Rohan, V. Lukeš, Homogenization of the acoustic transmission through a perforated layer, Journal of Computational and Applied Mathematics 234 (6) (2010) 1876–1885.
- [19] J.-J. Marigo, A. Maurel, Homogenization models for thin rigid structured surfaces and films, The Journal of the Acoustical Society of America 140 (1) (2016) 260–273.